The membrane skeleton of erythrocytes
A percolation model

Michael J. Saxton
Plant Growth Laboratory, University of California, Davis, California 95616, and Laboratory of Chemical Biodynamics, Lawrence Berkeley Laboratory, University of California, Berkeley, California 94720 USA

ABSTRACT The spectrin network on the cytoplasmic surface of the erythrocyte membrane is modeled as a triangular lattice of spectrin tetramers. This network obstructs lateral diffusion of proteins and provides mechanical reinforcement to the membrane. These effects are treated in a systematic and unified manner in terms of a percolation model. The diffusion coefficient is obtained as a function of the fraction of normal spectrin tetramers for both static and fluctuating barriers. The elasticity of the network is calculated as a function of the fraction of normal spectrin and the ratio of bending to stretching energies. For static barriers, elasticity and lateral diffusion are incompatible: if a network is connected enough to be elastic, it is connected enough to block long-range lateral diffusion. The elasticity and the force required for mechanical breakdown go to zero at the percolation threshold; experimental evidence suggests the existence of a stability threshold at or near the percolation threshold. The model is qualitatively applicable to other cells with membrane skeletons, such as epithelial cells, in which localization of membrane proteins is essential to differentiation.

INTRODUCTION

A network of spectrin and associated proteins is attached to the cytoplasmic surface of the erythrocyte plasma membrane. This network, the membrane skeleton, restricts the lateral diffusion of membrane proteins and provides mechanical reinforcement to the membrane (Sheetz, 1983), affecting both the deformability and the mechanical stability of the membrane (Chasis and Mohandas, 1986). In erythrocytes, the function of the membrane skeleton is mechanical reinforcement; in other cells, such as polarized epithelial cells, the function is restriction of the lateral diffusion of membrane proteins. The effects of the membrane skeleton on lateral diffusion, elasticity, and mechanical breakdown are described in terms of a percolation model. This model systematizes and unifies long-held views (Steck, 1974; Cherry et al., 1976) of the effects of the spectrin network.

In the normal erythrocyte, spectrin dimers associate head-to-head to form tetramers of length 200 nm fully extended; in the membrane skeleton, the end-to-end distance is $\simeq$76 nm. Actin and band 4.1 link the tetramers into a network; actin oligomers form the nodes of the network, and band 4.1 reinforces the association of spectrin with actin. Spectrin is bound to the anion transport protein band 3 by ankyrin, and to glycophorin by band 4.1. These connections to integral proteins attach the spectrin network to the cytoplasmic surface of the membrane (Sheetz, 1983; Goodman et al., 1988; Bennett, 1989). At 37°, ~20% of the band 3 dimer is bound to the spectrin network; the rest is free to rotate, but its lateral diffusion is hindered by the spectrin network (Tsuji et al., 1988). The effect on diffusion is significant: the diffusion coefficient of band 3 in normal erythrocytes is ~1/50 of the value in spectrin-free spherocytic mouse cells (Sheetz et al., 1980). Lipid diffusion is not significantly affected by the presence of spectrin (Bloom and Webb, 1983). Electron microscopy of stretched erythrocytes has shown that 80–90% of the spectrin is organized into a triangular lattice. Not all nodes have exactly six spectrin molecules attached, and higher oligomers of spectrin are present in low concentrations, but on the average the structure is well represented by a triangular lattice (Liu et al., 1987; Shen, 1989).

In erythrocytes, the membrane skeleton stabilizes the membrane against mechanical stress. This stabilization is essential if erythrocytes of diam 8 μm are to pass through capillaries of diam 2–3 μm repeatedly.

Many types of hereditary hemolytic anemia have been traced to defects in specific regions of proteins of the membrane skeleton, or to deficiencies in the amount of normal protein. These abnormalities prevent normal association of spectrin dimers into tetramers, or association of spectrin tetramers with other proteins, leading to abnormalities in shape and to fragmentation (Zail, 1986; Palek, 1987; Clark and Wagner, 1989). For example, in a family with hereditary elliptocytosis, as the amount of defective α-spectrin increased, the amount of spectrin tetramer

Address correspondence to Dr. Saxton, Plant Growth Laboratory, University of California, Davis, CA.

decreased and the mechanical stability of the membrane decreased (Lane et al., 1987). Agre et al. (1985) found that, in hereditary spherocytosis, as the spectrin content of the erythrocyte decreased, the severity of the disease increased. Here the spectrin molecule was normal but the amount of spectrin was low.

The membrane skeleton is modeled as an incomplete triangular lattice (Fig. 1) in which nodes represent actin oligomers, bonds represent normal spectrin tetramers, and missing bonds represent defective tetramers (Tsuji and Ohnishi, 1986). Defective tetramers include missing tetramers, single dimers, and dissociated dimer pairs. To find the diffusion coefficient, we take the tetramers to be barriers to diffusion and calculate their effect on diffusion as described earlier (Saxton, 1989*a*). To find the elasticity, we take the tetramers to be springs, and calculate the shear modulus of the lattice. The percolation model gives the diffusion coefficient and shear modulus as a function of the fraction b of intact bonds.

The model is illustrated in Fig. 1, in which bonds in a triangular lattice are cut at random. The elasticity of the network depends on paths along the bonds. As bonds are cut, the elasticity decreases, but above the percolation threshold, there is at least one continuous path extending across the network, and the elastic modulus is nonzero. Below the percolation threshold, there are only disconnected clusters of bonds, and the elasticity is zero. The percolation threshold for this lattice is $b_c = 2 \sin(\pi/18) = 0.347$ (Stauffer, 1985; Feder, 1988). The effect on diffusion depends on the gaps in the network. Initially, diffusion is highly restricted. As bonds are cut, the gaps grow larger, and the range of diffusion increases. Below the percolation threshold, the gaps extend across the entire network, and diffusion over the entire network is possible, though at a reduced rate. As still more bonds are cut, the paths for diffusion become less tortuous, and the diffusion coefficient increases.

Potential applications of the model include the changes in diffusion and elasticity during cellular development, and the effects of abnormalities in proteins of the membrane skeleton, either genetic defects (Clark and Wagner, 1989) or defects due to oxidative damage in stored erythrocytes (Wolfe et al., 1986) and in sickle cell anemia (Schwartz et al., 1987).

METHODS

Calculations of the diffusion coefficient for static barriers were carried out using the algorithm described earlier (Saxton, 1989*a*). The

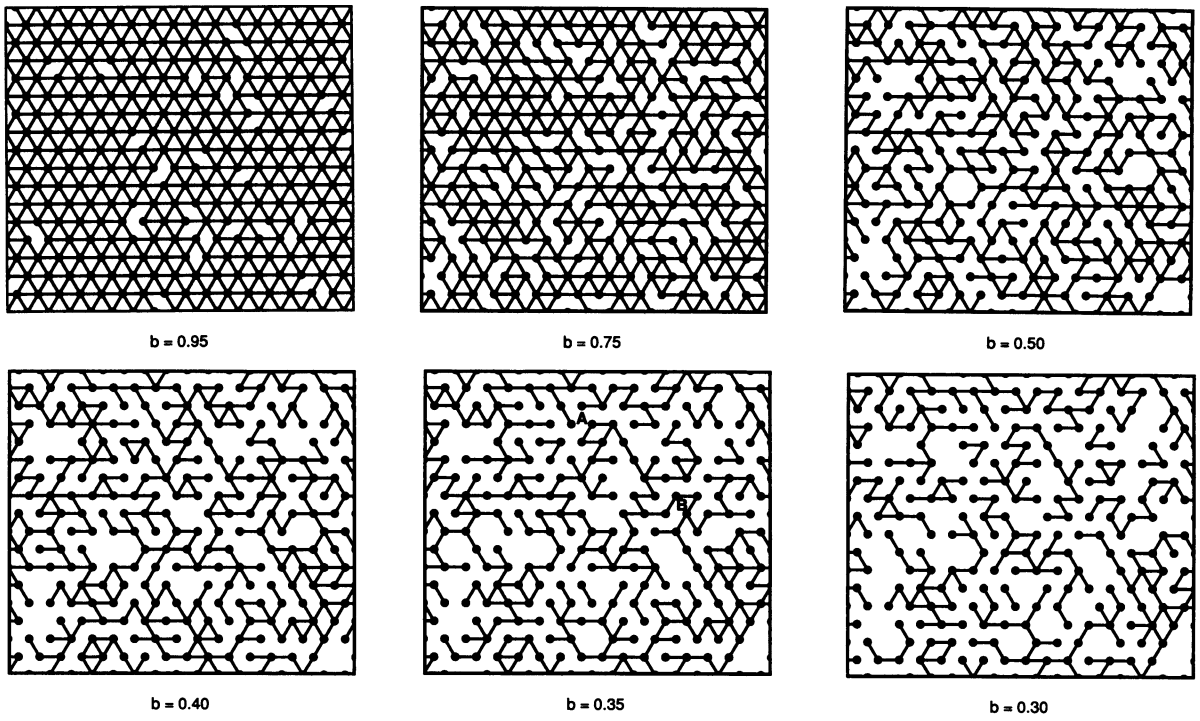

FIGURE 1 The erythrocyte membrane skeleton modeled as an incomplete triangular lattice. Bonds represent normal spectrin tetramers, missing bonds represent defective tetramers, and nodes represent actin oligomers. Bonds are removed randomly, and the fraction of bonds present is b. Note that in this example, when $b = 0.35$, just above the percolation threshold, there is no connected path of bonds from top to bottom, but adding one bond at A would connect top to bottom. There are several connected paths from left to right, but cutting one bond at B would disconnect left from right.

distance-dependent diffusion coefficient was obtained from these results as described earlier (Saxton, 1989*b*). Briefly, a point tracer executes a random walk on a honeycomb lattice with a fraction b of bonds blocked. The mean-square displacement $\langle r^2 \rangle$ of the tracer is found as a function of time, and the concentration-dependent, distance-dependent diffusion coefficient is obtained from $D^*(b, r) = \langle r^2 \rangle / t$. The limit of $D^*(b, r)$ as $t \rightarrow \infty$ is the usual diffusion coefficient, apart from a logarithmic correction discussed earlier (Saxton, 1989*a*, *b*). A 201 × 201 honeycomb lattice was used, with periodic boundary conditions. At each value of b, for short runs (100–500 time steps), the mean-square displacement was averaged over 100 different configurations of randomly blocked bonds and 1,000 different random walks per bond configuration. For the longest runs (150,000 time steps), 50 or 100 configurations of bonds were used, and 100 different random walks per bond configuration. The statistical error is illustrated in Figs. 3, *a* and *b*, where individual data points are plotted for several independent runs for $b = 0.2$.

Calculations for transient barriers were carried out similarly. Bonds in the honeycomb lattice are randomly assigned to two classes; a fraction $1 - b$ is permanently open, and a fraction b is transiently open. Permanently open bonds correspond to paths obstructed by defective spectrin tetramers, which are assumed to have no effect on diffusion. Transiently open bonds correspond to paths obstructed by normal spectrin tetramers. These paths are normally closed, but at each time step they open with a probability $1/\tau$ and remain open for one time step. Here τ is the characteristic time for transitions in the state of the barrier. As before, a point tracer executes a random walk on this lattice, and the diffusion coefficient is obtained. Calculations for Fig. 2 were carried out on a 201 × 201 honeycomb lattice for 50,000 time steps, with 100 bond configurations and 500 random walks per bond configuration. Calculations for Fig. 3 were carried out for 100–1,000 bond configurations, and 500 random walks per configuration.

The shear modulus was calculated by a modification of the method of Feng and Sen (1984). A 40 × 40 rectangular section of a triangular lattice is constructed, and periodic boundary conditions are imposed in one direction, forming a cylinder. A small shear displacement (typically 0.001 lattice constants) is applied to the boundary points along the edges of the cylinder, and the lattice points are allowed to relax to mechanical equilibrium. Then a loop is executed in which a fixed number of randomly chosen bonds is cut (typically 25), the lattice points are allowed to relax, and the shear modulus is calculated from the force on the boundary points.

The elastic energy function is given in Eq. 3. Relaxation to mechanical equilibrium is by a conjugate-gradient minimization method (Press et al., 1986), with a modified convergence test. The criterion for convergence was that the maximum magnitude of the x- or y-component of force exerted on any point by a nearest neighbor must be $< 1 \times 10^{-9}$ (compared with an initial force on a boundary point of 6×10^{-5}). All calculations were done in double precision. Calculations were done for 25 repetitions (for $D_\perp > 0$) or 50 repetitions (for $D_\perp = 0$). The statistical error is illustrated in Fig. 5 for $d = 0.01$; individual data points are plotted for two independent calculations (25 repetitions each) for a 40 × 40 lattice, and one calculation (25 repetitions) for a 50 × 50 lattice.

RESULTS

The Monte Carlo calculations yield the diffusion coefficient and the shear modulus as a function of the fraction b of intact spectrin tetramers. Here, b is proportional to the area density of normal spectrin tetramers, and is obtained from the observed ratio of spectrin to band 3, and the fraction of spectrin unable to associate normally (Saxton, 1989*a*). In the normal erythrocyte, $b \simeq 0.95$ (Palek and Lux, 1983). All results, whether calculations of diffusion for the honeycomb lattice or calculations of elasticity for the triangular lattice, are stated in terms of b. The diffusion coefficient is normalized to one for $b = 0$, and the elastic modulus is normalized to one for $b = 1$.

Diffusion in the presence of static barriers

In the diffusion problem, intact spectrin tetramers are assumed to act as barriers to protein diffusion; defective tetramers (dissociated dimer pairs, single dimers, and missing tetramers) allow proteins to diffuse freely from triangle to adjacent triangle in the lattice (Tsuji and Ohnishi, 1986). As demonstrated recently (see Fig. 1 of Saxton, 1989*a*), diffusion in the presence of a triangular lattice of barriers is equivalent to a random walk on bonds of the honeycomb lattice, which is the dual of the triangular lattice. Diffusion therefore shows a percolation threshold: the diffusion coefficient decreases monotonically with b, and goes to zero at the percolation threshold for bond percolation on the honeycomb lattice, $b_c = 0.347$. If $b > b_c$, the honeycomb lattice is disconnected enough that long-range diffusion is blocked. Monte Carlo results are shown in Fig. 2.

It is assumed that spectrin tetramers act purely as barriers to diffusion, obstructing the cytoplasmic domain of membrane proteins. An alternative view is that lateral diffusion is hindered by transient binding of membrane proteins to immobile elements of the membrane skeleton. Evidence in support of a binding model is presented by Golan (1989); the models are reviewed by Saxton (1990).

A pure binding model appears implausible because it would require spectrin to be suspended above the membrane so that diffusing proteins could pass beneath it freely. But a pure obstruction model appears implausible in view of the known interactions among integral proteins in the erythrocyte. Both effects are likely to be significant. Nevertheless, it is useful to model the pure mechanisms to help disentangle their contributions.

Diffusion in the presence of fluctuating barriers

The preceding picture holds if the network is static. But tetramers are in equilibrium with dimer pairs, and the spectrin molecules may undergo conformational fluctuations that allow diffusing proteins to pass under them (Koppel et al., 1981; Sheetz, 1983). If the barriers fluctuate between open and closed states, there is no percolation threshold, and diffusion may occur for any fraction of barriers.

The problem is still equivalent to bond percolation on the honeycomb lattice, and Monte Carlo calculations can be used to obtain the diffusion coefficient as a function of b and of the relaxation time τ for transitions between blocked and unblocked states. In these calculations, there are two classes of bonds, transiently open bonds and permanently open bonds. Transiently open bonds, present at a concentration b, correspond to a path blocked by a normal tetramer. These bonds are normally closed, but open with a probability $1/\tau$ in each time step. Permanently open bonds, present at a concentration $1 - b$, correspond to an unobstructed path, in which the spectrin tetramer is defective.

Results for static and fluctuating barriers are shown in Fig. 2. The static limit $\tau = \infty$ is applicable when the diffusion measurement is much faster than the relaxation time τ. When the measurement is slower than the relaxation time, the curves for finite τ are appropriate. Only in the limit $\tau \rightarrow \infty$ is diffusion completely blocked above the percolation threshold; this corresponds to a spectrin molecule that is, on the time scale of the measurement, always bound to the membrane and always in the tetrameric form.

In Fig. 2, the effective-medium curve

$$D^* = 1 - 3b \tag{1}$$

agrees well with the Monte Carlo results except near the percolation threshold (Saxton, 1989*a*). The effective-medium percolation threshold is 1/3; the exact value is 0.347 (Stauffer, 1985). Note that

$$D^*(1) = 1/\tau. \tag{2}$$

That is, if the spectrin network is complete, diffusion is equivalent to a random walk on a complete honeycomb lattice, but only a fraction $1/\tau$ of the jumps is successful.

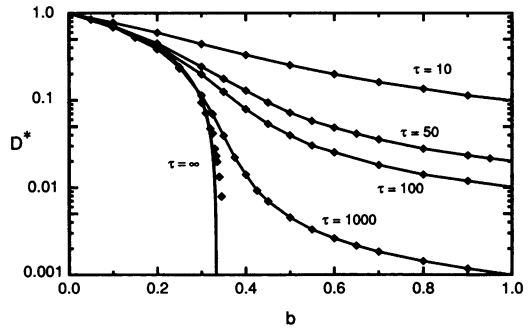

FIGURE 2 Diffusion coefficient D^* as a function of the fraction b of normal spectrin tetramer, for the indicated time constants τ. The diffusion coefficient is normalized to one for all spectrin in dimeric form. Points are from Monte Carlo calculations; the curve for $\tau = \infty$ is the effective-medium value (Eq. 1); the other curves are guides for the eye.

The diffusion coefficient of band 3 in a normal mouse erythrocyte is 1/50 that in a spectrin-free spherocytic mouse erythrocyte (Sheetz et al., 1980), so that by Eq. 2, $\tau \simeq 50$. Now τ is the ratio of the relaxation time τ_B of the barrier to the jump time τ_J of the diffusing particle, and τ_J is the time required for a particle to diffuse one bond length ℓ_{HC} on the honeycomb lattice, that is, the time for a particle to diffuse from the center of one triangle to the center of an adjacent triangle in the spectrin network, in the absence of barriers. So $\tau_J = \ell_{HC}^2/4D$, where $\ell_{HC} = 44$ nm, and $D = 0.25\ \mu m^2/s$, the observed value in a spectrin-free mouse erythrocyte (Sheetz et al., 1980). Then $\tau_J = 2$ ms, so that $\tau = 50$ corresponds to a relaxation time $\tau_B = 100$ ms. Reasons for the discrepancy between τ_B and the observed value in bulk solution were discussed earlier (Saxton, 1989*a*).

Many experiments have shown that alteration of the structure of the spectrin network has a major effect on lateral diffusion of integral proteins (Sheetz, 1983; Tsuji and Ohnishi, 1986; Golan, 1989). Agents dissociating the network, such as polyphosphates or the 72-kD fragment of ankyrin, increase the diffusion coefficient of integral proteins. Agents increasing association, such as ankyrin, polyamines, diamide, or high ionic strength, decrease the diffusion coefficient.

It would be useful to have measurements of lateral diffusion in which b and τ are varied independently. To vary b, cells with defective spectrin could be used, or normal cells treated with a sulfhydryl blocking reagent (Smith and Palek, 1983). To vary τ, agents such as 2,3-diphosphoglycerate could be used; these increase the rate of dissociation and association (Sheetz and Casaly, 1980).

Distance dependence of the lateral diffusion coefficient

The usual concentration-dependent diffusion coefficient $D^*(b)$ can be generalized to include the effect of the distance over which diffusion is measured. The basic physical idea is that a label is produced at $t = 0$, and its diffusion is then measured over a distance r. In fluorescence photobleaching recovery experiments, r is of the order of the radius of the photobleached area, typically 1 μm or more, whereas in measurements by excimer formation or fluorescence quenching, r is of the order of the average initial separation of interacting species, typically 1–10 nm. The effects of obstacles on diffusion may be much different in these two cases (Eisinger et al., 1986; Saxton, 1989*b*). The distance-dependent diffusion coefficient $D^*(b, r)$ can be obtained from Monte Carlo calculations (Saxton, 1989*b*).

Numerical values for static barriers are shown in Fig. 3, *a* and *b*. If no bonds are blocked, $D^*(0, r) = 1$ for all r.

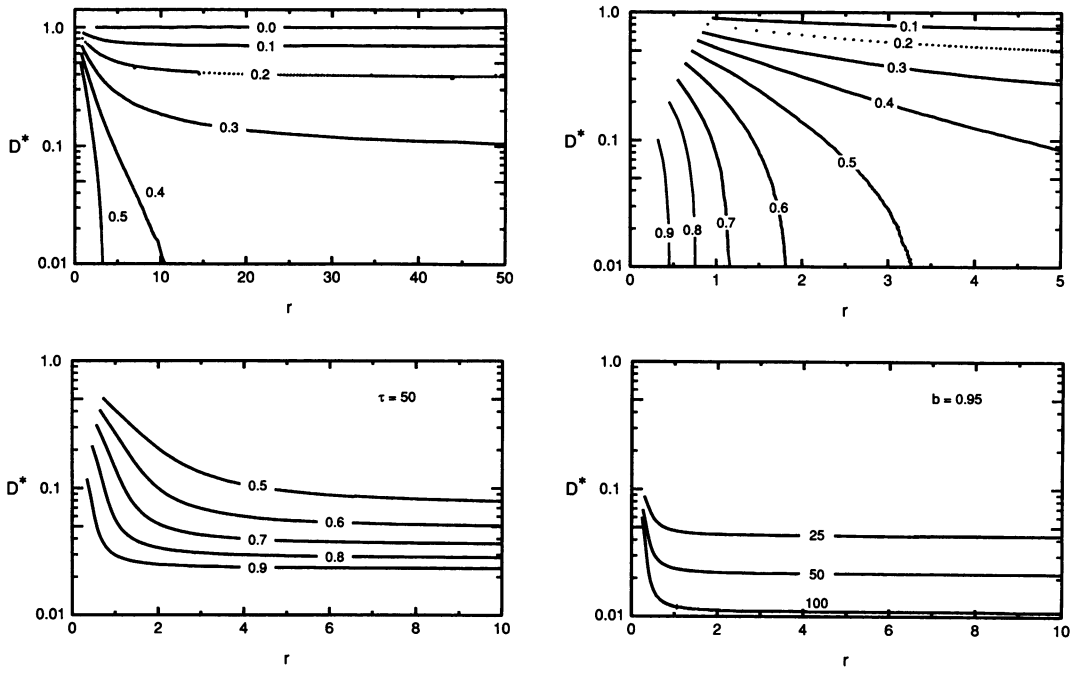

FIGURE 3 Distance dependence of the diffusion coefficient D^* at the indicated concentrations of normal spectrin tetramers for diffusion of a point tracer in the presence of static or transient barriers. The unit of length is ℓ_{HC}, the lattice spacing for the honeycomb lattice. (*a*, *b*) Static barriers. To illustrate the statistical error, individual data points are shown for $c = 0.2$, for eight different runs of four different lengths. (*c*) Transient barriers. For $\tau = 50$, the value estimated in the text, $D^*(r)$ is given for the indicated values of b. (*d*) Transient barriers. For $b = 0.95$, the value for normal erythrocytes, $D^*(r)$ is given for $\tau = 25$, 50, and 100.

At low concentrations of blocked bonds, $D^*(b, r)$ approaches a limiting value $D^*(b)$ as $r \rightarrow \infty$; the Monte Carlo results in Fig. 2 for $\tau = \infty$ are those limits. At high concentrations of blocked bonds, above the percolation threshold, $D^*(b, r)$ decreases with r, and goes to zero at some finite distance. This is the range of local diffusion, and decreases as more bonds are blocked. A simple formula for this range has been obtained (Saxton, 1989*a*, Eq. 5).

Numerical values for transient barriers are shown in Fig. 3 *c* for $\tau = 50$ and a range of values of b, and in Fig. 3 *d* for $b = 0.95$, the value for the normal erythrocyte, for a range of values of τ. Note that $D^*(b, r)$ reaches its limiting value very quickly, particularly for large values of b.

In Fig. 3, r is in units of ℓ_{HC}, the lattice spacing of the honeycomb lattice; this is related to ℓ_{TRI}, the lattice spacing of the triangular lattice, by $\ell_{HC} = \ell_{TRI}/\sqrt{3}$. So if the length of the unstretched spectrin tetramer is $\ell_{TRI} = 76$ nm (Sheetz, 1983), then $\ell_{HC} = 44$ nm. For static barriers, then, if $b = 0.6$, D^* goes to zero at $r \simeq 1.8 \simeq 79$ nm. A diffusion measurement by excimer formation would show diffusion, at a reduced rate, whereas in a photobleaching measurement both the diffusion coefficient and the fractional recovery would be practically zero. For transient barriers, if $b = 0.6$ and $\tau = 50$, D^* reaches its limiting value at $r \simeq 5 \simeq 220$ nm, and a photobleaching measurement would yield that value.

Elasticity

Using the same model of an incomplete triangular lattice of spectrin tetramers, we can calculate the shear modulus of the network as a function of the fraction of intact spectrin tetramers. Intact tetramers correspond to springs, whereas defective tetramers are counted as missing springs. Monte Carlo calculations yield the shear modulus μ^* as a function of the fraction b of springs present and the ratio $d = D_\perp/D_\parallel$ of the elastic energy coefficients for bending $D_\perp$, and for stretching, $D_\parallel$.

The shear modulus is calculated because experimental results are available and the calculation is simpler. The bending modulus is of great interest (Nelson et al., 1988), but the computer time required for three-dimensional calculations is large. For a randomly cut triangular lattice, all the elastic moduli are expected to go to zero at the same percolation threshold.

For these calculations, we assume that the elastic energy of a spectrin tetramer is (Schwartz et al., 1985;

Arbabi and Sahimi, 1988)

$$E = (D_\parallel/2)\sum_{\langle ij\rangle} g_{ij}[(\mathbf{u}_i - \mathbf{u}_j)\cdot\hat{R}_{ij}]^2 + (D_\perp/2)\sum_{\langle jik\rangle} g_{ij}g_{ik} \cdot [(\mathbf{u}_i - \mathbf{u}_j)\times\hat{R}_{ij} - (\mathbf{u}_i - \mathbf{u}_k)\times\hat{R}_{ik}]^2 . \quad (3)$$

Here $\mathbf{u}_i$ is the displacement of site i from its equilibrium position, $\hat{R}_{ij}$ is a unit vector from site i to site j, and $g_{ij} = 1$ if sites i and j are connected, and 0 if not. The first sum represents the stretching energy; the second sum, the bending energy. The first sum is over pairs of nearest-neighbor sites; the second sum is over triplets in which the $j - i$ and $i - k$ bonds form an angle with vertex i.

This form of the elastic energy is often used in the percolation literature. The stretching term is a harmonic function of the displacement; for small displacements, the bending term is quadratic in the deviation of the angle *jik* from its equilibrium value. We thus assume that the elasticity is purely energetic in origin, and neglect the entropic contribution (Mark, 1981).

Fig. 4 *a* shows the elastic energy of an intact lattice as one point is displaced along a bond. For a given displacement, the bending energy ($D_\parallel = 0$; $D_\perp = 1$) is much larger than the stretching energy ($D_\parallel = 1$; $D_\perp = 0$). So the appropriate range of $D_\perp$ is $D_\perp \ll D_\parallel$, particularly for a molecule as flexible as spectrin. We take $D_\parallel = 1$ and $D_\perp \leq 0.2$. Fig. 4 *b* shows a contour plot of the elastic energy for displacements of a point connected to the lattice by a single bond.

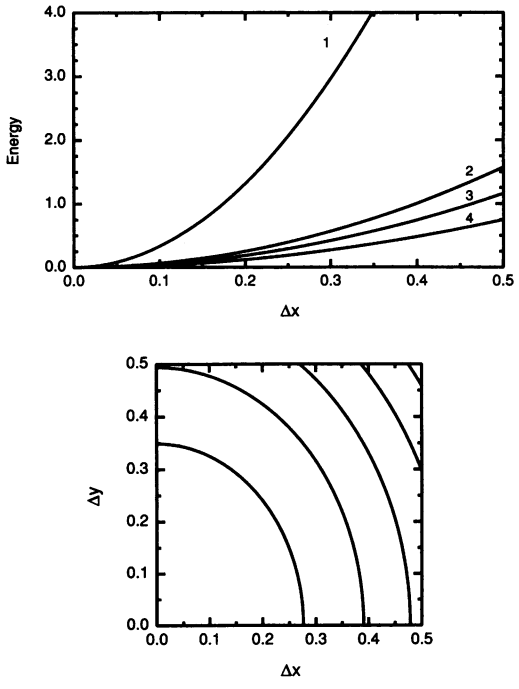

FIGURE 4 (*a*) Elastic energy (arbitrary units) as a function of the displacement of one point from equilibrium. No bonds are cut, and the displacement is along a bond. (1), Bending energy only ($D_\parallel = 0$; $D_\perp = 1$). (2), $D_\parallel = 1$; $D_\perp = 0.1$. (3), $D_\parallel = 1$; $D_\perp = 0.05$. (4), Stretching energy only ($D_\parallel = 1$; $D_\perp = 0$). (b) Contour plot of the elastic energy for displacements Δx, Δy of a point connected to the lattice by a single bond. Here $d = 0.01$, the contour interval is 0.1, and the unit of energy is the same as in Fig. 4 *a*.

Values of $\mu^*(b, d)$ are shown in Fig. 5. If $D_\perp > 0$, the shear modulus goes to zero at the percolation threshold for the triangular lattice, $b_c = 0.347$. If $D_\perp = 0$, the percolation threshold shifts to the value for rigidity percolation (Feng et al., 1985), $b_r \simeq 0.642$ (Roux and Hansen, 1988).

Rigidity percolation

In rigidity percolation, only bond-stretching forces are included. The percolation threshold is then higher because there are "floppy regions" which are connected but cannot transmit an elastic force. Consider two rigid regions connected by a single bent pair of bonds (Fig. 5, *inset*). The regions are connected, but over a short distance they can be pulled apart with zero force because the bond has no resistance to bending. To connect these regions rigidly, more bonds are needed (Feng et al., 1985; Garboczi and Thorpe, 1985). The percolation threshold is therefore much larger, $b_r \simeq 0.642$ for the triangular lattice (Roux and Hansen, 1988) instead of $b_c = 0.347$ for ordinary percolation. Between these concentrations, the network is connected enough to block diffusion but not connected enough to be rigid.

Comparison with experiment

No experimental value for d is available. The spectrin molecule is very flexible (Elgsaeter et al., 1986); a

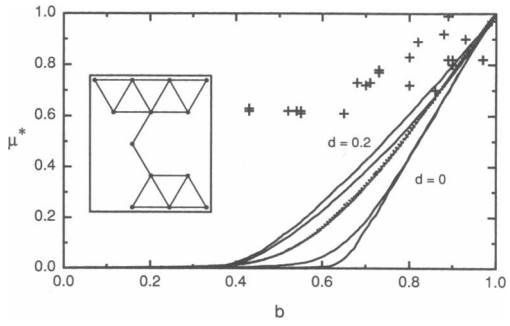

FIGURE 5 Normalized shear modulus μ^* as a function of b. *(Lines and points)* Calculated values for the ratios $d = 0$, 0.001, 0.01, 0.1, 0.2 of the bending energy coefficient to the stretching energy coefficient. To illustrate the statistical error, individual data points from three independent calculations are plotted for $d = 0.01$, two for a 40 × 40 lattice and one for a 50 × 50 lattice. *(Crosses)* Experimental values (Waugh, 1987; Waugh and Agre, 1988) for erythrocytes from patients with hereditary hemolytic anemia. Note that no patients were found with $b < 0.40$. *(Inset)* Rigidity percolation (see text).

structural model of the spectrin dimer includes many hinge points (Speicher and Marchesi, 1984). But evidence from the self-association of spectrin in bulk solution indicates that the bending energy is nonzero (Shahbakhti and Gratzer, 1986). The bending energy in bulk solution has been estimated to be of the order of magnitude of the thermal energy or less (Stokke et al., 1985), and the free energy of shear deformation has been estimated to be slightly larger than the thermal energy (Waugh, 1987).

Measurements of the shear modulus of individual erythrocytes by micropipette aspiration (Waugh, 1987; Waugh and Agre, 1988) showed that the shear modulus is proportional to the amount of spectrin present (Fig. 5). Chabanel et al. (1989) found, surprisingly, an increase in the elasticity of elliptocytic erythrocytes as the fraction of spectrin dimer increased.

At the lowest values of b measured, the experimental results may be affected by the fact that the entire population of erythrocytes is used in spectrin assays, but knly a subpopulation of more intact cells is suitable for elasticity measurements. The measured values may therefore be upper bounds, for the least-damaged cells in the sample (Waugh, 1987; Waugh and Agre, 1988). In the samples most affected, <15% of the cells were suitable for measurement (Waugh, 1987). But this cannot explain the disagreement for higher values of b. The discrepancy between calculated and observed values is real; the experimental results cannot be reproduced using the elastic energy function of Eq. 3.

The use of a different potential energy function for the spectrin molecule may lead to better agreement, though the percolation model implies that for any choice of the potential energy function, the elastic modulus must go to zero at the percolation threshold. The time scale of the measurements may be important; the values of μ^* shown are for a static network (that is, it is assumed that the network does not change during the time required for a measurement). The assumption that the membrane skeleton is a simple triangular lattice may require modification, as discussed later.

Mechanical breakdown

The shear modulus describes the response to low shear; at high shear, breakdown of the network may occur. Chasis and Mohandas (1986) presented a model of the membrane skeleton in which deformability corresponds to reversible extensions of spectrin springs; fragmentation results when spectrin is stretched to the point at which spectrin-spectrin or spectrin-actin-band 4.1 connections are broken. A similar distinction is made in the percolation literature, between elasticity models and breakdown models.

Models of mechanical breakdown (Beale and Srolovitz, 1988; Meakin, 1987) resemble elasticity models, except that the springs have a threshold: if a spring is stretched beyond its threshold, it breaks. Beale and Srolovitz (1988) used an incomplete triangular lattice of springs with central forces only ($D_\perp = 0$). In their calculations, a small uniform strain is applied in one direction, and the system is allowed to relax to mechanical equilibrium. If any spring is stretched beyond its threshold, the spring is broken and the system is again allowed to relax to equilibrium. This process is continued with increasing strain until the network breaks in two. The calculations yield the strain for initial failure and the strain for macroscopic breakdown, as a function of the fraction of springs present.

The strain required for breakdown, like the elasticity, goes to zero at the percolation threshold of the lattice (Bergman, 1986; Beale and Srolovitz, 1988). As b increases above b_c, the force required for breakdown increases, so that the observed threshold for breakdown depends on the applied force.

DISCUSSION

A unified picture of diffusion and elasticity

We combine the previous results into Fig. 6, showing the shear modulus and the long-range diffusion coefficient for static barriers as a function of the concentration b of intact spectrin tetramers.

Suppose that we start with a complete network $b = 1$. The network has unit elasticity, and lateral diffusion is blocked. A protein cannot move beyond the triangle in which it is trapped, though if it is unbound it is free to undergo rotational diffusion. If a few bonds are cut, the elasticity decreases, as shown in Fig. 6, and local diffusion

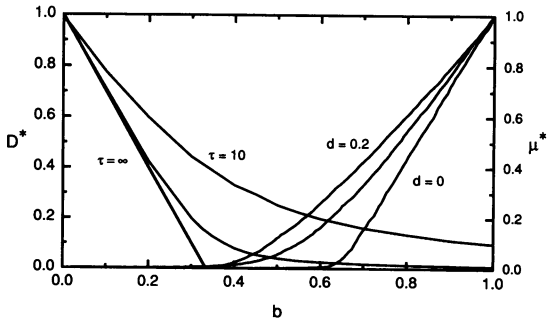

FIGURE 6 (*Left*) Diffusion coefficient D^* from Monte Carlo calculations as a function of the fraction b of spectrin tetramer, for time constants for bond opening $\tau = 10, 100, \infty$. (*Right*) Shear modulus μ^* as a function of b. Monte Carlo values for ratios $d = 0, 0.01, 0.2$ of the bending energy coefficient to the stretching energy coefficient.

becomes possible, as shown in Fig. 3. As more bonds are cut, the elasticity decreases further, and the range of local diffusion continues to increase. At the percolation threshold, the elasticity of the network goes to zero, and paths for long-range diffusion begin to appear, extending over the entire surface of the cell. As still more bonds are cut, more long-range paths appear, and the long-range diffusion coefficient increases. Finally, at $b = 0$, there is free diffusion over all distances.

A normal spectrin tetramer corresponds to a spring that is present in the elasticity problem, and to a path that is blocked in the diffusion problem. The percolation thresholds for the two problems are thus complementary. For static barriers, then, mechanical reinforcement and lateral diffusion of proteins are incompatible. If a lattice is connected enough to be elastic over long distances, it is connected enough to block diffusion over long distances. For transient barriers, the incompatibility is not as strict; diffusion is allowed at any concentration of spectrin, but at a rate determined by the fluctuations in the barriers. Brain spectrin is much stiffer than erythrocyte spectrin (Coleman et al., 1989). So, whereas a network of erythrocyte spectrin might allow diffusion at a reduced rate, a similar network of brain spectrin might block diffusion completely.

The relation of elasticity and lateral diffusion was shown in experiments on tethers formed by erythrocytes in a flow chamber (Berk et al., 1989). The tethers lose shear rigidity, and lateral diffusion is greatly enhanced, implying that the lipid bilayer in the tethers is separated from the membrane skeleton.

The prevention of lateral diffusion may be physiologically important. Localization of membrane components is essential to the differentiation and function of many types of cells, including epithelial cells and nerve cells (Almers and Stirling, 1984).

Several mechanisms may be involved in the polarization of epithelial cells: the transport of newly synthesized protein to the appropriate membrane domain, obstruction of diffusion by the tight junction, and obstruction of diffusion by the membrane skeleton (Fleming, 1987). But Ojakian and Schwimmer (1988) demonstrated that some proteins can be localized in epithelial cells even in the absence of a tight junction.

There is much evidence that the membrane skeleton is involved in polarization. Proteins cross-reactive with erythrocyte band 3, spectrin, and ankyrin are present in basolateral membranes of certain kidney cells (Drenckhahn et al., 1985). Spectrin, ankyrin, and Na^+, K^+ ATPase colocalize in basolateral membranes of those cells (Drenckhahn et al., 1985; Koob et al., 1987). Ankyrin binds to the ATPase (Koob et al., 1987). And during the development of a continuous monolayer of MDCK cells, when cell–cell contact becomes extensive, a polarized distribution of ATPase develops at the basolateral membrane at the same time as a spectrin layer forms there (Nelson, 1989). Jesaitis and Yguerabide (1986) found that half of the ATPase is mobile over micrometer distances, as measured in fluorescence photobleaching recovery experiments, but Nelson (1989) argues that the membrane skeleton had not yet formed in the small colonies of cells used in those measurements.

A very similar picture of the membrane skeleton of nerve cells is emerging (Goodman et al., 1988).

Death at the percolation threshold?

Mechanical breakdown of erythrocytes is physiologically important; the basic indication of certain types of hereditary hemolytic anemia is the presence of fragmented erythrocytes (Zail, 1986; Palek, 1987; Clark and Wagner, 1989). In hereditary hemolytic anemia, it is well established that the fragility of the erythrocyte is increased by defects leading to the inability to form the normal amount of tetramer (Lane et al., 1987). As demonstrated in cases of hereditary spherocytosis, the less tetramer present, the more fragile the cell, and the more severe the illness (Agre et al., 1985; Chasis et al., 1988). The response of erythrocytes to shear forces in the laboratory is used to characterize cases of hereditary hemolytic anemia (Mohandas, 1988; Waugh and Agre, 1988).

Experimental evidence suggests the existence of a stability threshold at or near the percolation threshold $b_c = 0.347$ for the triangular lattice. In trypsin-treated erythrocyte ghosts, the stability threshold was between 28% and 45% spectrin (Shields et al., 1987). Waugh and Agre (1988) measured the shear modulus of erythrocytes from patients with hereditary spherocytosis and hereditary elliptocytosis, and noted the possibility of a threshold: all cells measured had at least 40% spectrin (Fig. 5). In cases of hereditary spherocytosis, the lowest concentrations of spectrin observed were 45–55%, and for these four patients the disease was nearly lethal (Agre et al., 1985). Chasis et al. (1988) measured the mechanical stability of erythrocytes of patients with hereditary spherocytosis. The stability was reduced, the reduction was correlated with spectrin content, and the authors state that "no patient has yet been identified with <30% of the normal spectrin content, and deficiencies of this magnitude may be lethal."

In the few cases in which $b < b_c$ (Saxton, 1989*a*), the fragility of the erythrocytes is extreme. In one case of hereditary pyropoikilocytosis (Peterson et al., 1987), $b = 0.27$. For these erythrocytes, the disintegration time under shear stress was 2.5 min; controls required 33 min. In a case of homozygous hereditary elliptocytosis (Evans et al., 1983), $b = 0.18$; the patient required frequent

transfusions. In the spherocytic mouse cells used in lateral diffusion measurements (Sheetz et al., 1980), spectrin is almost completely absent. The lifetime of these erythrocytes is 1.0 d; the lifetime of normal cells is 48 d. The fraction of reticulocytes was 91.2% in spherocytic mice, and 3.2% in normal mice (Bernstein, 1980). In the original spherocytic line, all homozygotes died within 24 h of birth (Joe et al., 1962).

Several complicating factors need to be considered. First, breakdown is likely to occur slightly above the percolation threshold. Just above b_c, the entire shear stress may be borne by a single bond (such as bond B in Fig. 1 *e*), and this bond may break. Second, the differences in protein defects in the various forms of hereditary hemolytic anemia may be significant. Third, the simple triangular lattice model is an approximation. Higher-order spectrin oligomers (Shen, 1989) may lead to long-distance cross-linking. Nonadjacent sites may also be cross-linked by association of normal spectrin dimers left dangling by defective partners. Entanglement of dangling spectrin dimers (Chabanel et al., 1989) may also be important. All of these associations may be permanent or transient.

Applicability to other geometries

The assumption that the spectrin network forms a triangular lattice simply determines the location of the percolation threshold. Other lattices would yield similar families of curves, going to zero at some other concentration of bonds. The results of this paper are thus qualitatively applicable to other cells with a membrane skeleton (Bennett et al., 1988), such as nerve (Goodman et al., 1988), kidney (Nelson, 1989), and muscle (Kunkel, 1989) cells.

In muscle cells, the membrane skeleton may provide mechanical reinforcement. Recent work on muscular dystrophy has implicated the protein dystrophin. Dystrophin is structurally similar to spectrin, as judged by its sequence, and it is localized near the plasma membrane. Dystrophin is present in normal muscle; it is absent in Duchenne muscular dystrophy; and it is abnormal in the less severe form, Becker's muscular dystrophy (Kunkel, 1989). If, as recent evidence suggests (Mandel, 1989), dystrophin forms a honeycomb lattice, the percolation threshold would be shifted from 0.347 to 0.653.

Relation to other models

The ionic gel model (Elgsaeter et al., 1986) includes three contributions to membrane properties: the elasticity of the spectrin network, spectrin–spectrin interactions, and the hydrogen ion tension. The percolation model treats the first of these, and takes into account the connectivity of the network. Eventually it may be possible to combine the two models.

If the elastic properties of the membrane skeleton are known as a function of spectrin concentration, this result can be used as an input to classical continuum mechanics (Evans and Skalak, 1980; Berk et al., 1989). At this point, the elastic properties of the lipid bilayer can be included.

What the percolation model contributes is a way to evaluate the effect of the connectedness of the membrane skeleton on elasticity and lateral diffusion. The major conclusions are (*a*) the incompatibility of lateral diffusion and mechanical reinforcement, partial if there are fluctuations in spectrin conformation or association, complete if there are not; and (*b*) the identification of the observed threshold for mechanical instability with the percolation threshold for the triangular lattice. Membrane skeletons of other cells with different lattice structures will show similar behavior, but at a different threshold.

I thank D.E. Golan, A. Tsuji, and R. E. Waugh for useful discussions, and R. W. Breidenbach, R. S. Criddle, J. C. Owicki, and the reviewers for comments on the manuscript.

This work was supported in part by National Institutes of Health grant GM38133.

Received for publication 7 August 1989 and in final form 12 February 1990.

REFERENCES

Agre, P., J. F. Casella, W. H. Zinkham, C. McMillan, and V. Bennett. 1985. Partial deficiency of erythrocyte spectrin in hereditary spherocytosis. *Nature (Lond.)*. 314:380–383.

Almers, W., and C. Stirling. 1984. Distribution of transport proteins over animal cell membranes. *J. Membr. Biol.* 77:169–186.

Arbabi, S., and M. Sahimi. 1988. Elastic properties of three-dimensional percolation networks with stretching and bond-bending forces. *Phys. Rev. B.* 38:7173–7176.

Beale, P. D., and D. J. Srolovitz. 1988. Elastic fracture in random materials. *Phys. Rev. B.* 37:5500–5507.

Bennett, V. 1989. The spectrin-actin junction of erythrocyte membrane skeletons. *Biochim. Biophys. Acta.* 988:107–121.

Bennett, V., J. Steiner, and J. Davis. 1988. Diversity in protein associations of the spectrin-based membrane skeleton of nonerythroid cells. *Protoplasma.* 145:89–94.

Bergman, D. J. 1986. Fracture and plasticity of random elastic networks near the rigidity threshold. *Ann. Isr. Phys. Soc.* 8:266–272.

Berk, D. A., R. M. Hochmuth, and R. E. Waugh. 1989. Viscoelastic properties and rheology. *In* Red Blood Cell Membranes: Structure, Function, Clinical Implications. P. Agre and J. C. Parker, editors. Marcel Dekker, Inc., New York. 423–454.

Bernstein, S. E. 1980. Inherited hemolytic disease in mice: a review and update. *Lab. Anim. Sci.* 30:197–205.

Bloom, J. A., and W. W. Webb. 1983. Lipid diffusibility in the intact erythrocyte membrane. *Biophys. J.* 42:295–305.

Chabanel, A., K.-L. P. Sung, J. Rapiejko, J. T. Prchal, J. Palek, S. C. Liu, and S. Chien. 1989. Viscoelastic properties of red cell membrane in hereditary elliptocytosis. *Blood.* 73:592–595.

Chasis, J. A., and N. Mohandas. 1986. Erythrocyte membrane deformability and stability: two distinct membrane properties that are independently regulated by skeletal protein associations. *J. Cell Biol.* 103:343–350.

Chasis, J. A., P. Agre, and N. Mohandas. 1988. Decreased membrane mechanical stability and in vivo loss of surface area reflect spectrin deficiencies in hereditary spherocytosis. *J. Clin. Invest.* 82:617–623.

Cherry, R. J., A. Bürkli, M. Busslinger, G. Schneider, and G. R. Parish. 1976. Rotational diffusion of band 3 proteins in the human erythrocyte membrane. *Nature (Lond.).* 263:389–393.

Clark, M. R., and G. M. Wagner. 1989. Disorders of the erythrocyte membrane. *In* The Hereditary Hemolytic Anemias. W. C. Mentzer and G. M. Wagner, editors. Churchill Livingstone, New York. 223–266.

Coleman, T. R., D. J. Fishkind, M. S. Mooseker, and J. S. Morrow. 1989. Contributions of the β-subunit to spectrin structure and function. *Cell Motil. Cytoskeleton.* 12:248–263.

Drenckhahn, D., K. Schlüter, D. P. Allen, and V. Bennett. 1985. Colocalization of band 3 with ankyrin and spectrin at the basal membrane of intercalated cells in the rat kidney. *Science (Wash. DC).* 230:1287–1289.

Eisinger, J., J. Flores, and W. P. Petersen. 1986. A milling crowd model for local and long-range obstructed lateral diffusion. *Biophys. J.* 49:987–1001.

Elgsaeter, A., B. T. Stokke, A. Mikkelsen, and D. Branton. 1986. The molecular basis of erythrocyte shape. *Science (Wash. DC).* 234:1217–1223.

Evans, E. A., and R. Skalak. 1980. Mechanics and Thermodynamics of Biomembranes. CRC Press, Boca Raton, FL. 254 pp.

Evans, J. P. M., A. J. Baines, I. M. Hann, I. Al-Hakim, S. M. Knowles, and A. V. Hoffbrand. 1983. Defective spectrin dimer-dimer association in a family with transfusion dependent homozygous hereditary elliptocytosis. *Br. J. Haematol.* 54:163–172.

Feder, J. 1988. Fractals. Plenum Press, New York. 283 pp.

Feng, S., and P. N. Sen. 1984. Percolation on elastic networks: new exponent and threshold. *Phys. Rev. Lett.* 52:216–219.

Feng, S., M. F. Thorpe, and E. Garboczi. 1985. Effective-medium theory of percolation on central-force elastic networks. *Phys. Rev. B.* 31:276–280.

Fleming, T. P. 1987. Trapped by a skeleton-the maintenance of epithelial membrane domains. *BioEssays.* 7:179–181.

Garboczi, E. J., and M. F. Thorpe. 1985. Effective-medium theory of percolation on central-force elastic networks. II. Further results. *Phys. Rev. B.* 31:7276–7281.

Golan, D. E. 1989. Red blood cell membrane protein and lipid diffusion. *In* Red Blood Cell Membranes: Structure, Function, Clinical Implications. P. Agre and J. C. Parker, editors. Marcel Dekker, Inc., New York. 367–400.

Goodman, S. R., K. E. Krebs, C. F. Whitfield, B. M. Riederer, and I. S. Zagon. 1988. Spectrin and related molecules. *CRC Crit. Rev. Biochem.* 23:171–234.

Jesaitis, A. J., and J. Yguerabide. 1986. The lateral mobility of the (Na^+,K^+)-dependent ATPase in Madin-Darby canine kidney cells. *J. Cell Biol.* 102:1256–1263.

Joe, M., J. M. Teasdale, and J. R. Miller. 1962. A new mutation (sph) causing neonatal jaundice in the house mouse. *Can. J. Genet. Cytol.* 4:219–225.

Koob, R., M. Zimmermann, W. Schoner, and D. Drenckhahn. 1987. Colocalization and coprecipitation of ankyrin and Na^+,K^+-ATPase in kidney epithelial cells. *Eur. J. Cell Biol.* 45:230–237.

Koppel, D. E., M. P. Sheetz, and M. Schindler. 1981. Matrix control of protein diffusion in biological membranes. *Proc. Natl. Acad. Sci. USA.* 78:3576–3580.

Kunkel, L. M. 1989. Muscular dystrophy: a time of hope. *Proc. R. Soc. Lond. B Biol. Sci.* 237:1–9.

Lane, P. A., R. L. Shew, T. A. Iarocci, N. Mohandas, T. Hays, and W. C. Mentzer. 1987. Unique alpha-spectrin mutant in a kindred with common hereditary elliptocytosis. *J. Clin. Invest.* 79:989–996.

Liu, S. C., L. H. Derick, and J. Palek. 1987. Visualization of the hexagonal lattice in the erythrocyte membrane skeleton. *J. Cell Biol.* 104:527–536.

Mandel, J. L. 1989. Dystrophin: the gene and its product. *Nature (Lond.).* 339:584–586.

Mark, J. E. 1981. Rubber elasticity. *J. Chem. Educ.* 58:898–903.

Meakin, P. 1987. A simple model for elastic fracture in thin films. *Thin Solid Films.* 151:165–190.

Mohandas, N. 1988. Measurement of cellular deformability and membrane material properties of red cells by ektacytometry. *In* Red Cell Membranes. S. B. Shohet and N. Mohandas, editors. Churchill Livingstone, New York. 299–320.

Nelson, D., T. Piran, and S. Weinberg. 1988. Statistical Mechanics of Membranes and Surfaces. World Scientific, Singapore. 261 pp.

Nelson, W. J. 1989. Development and maintenance of epithelial polarity: a role for the submembranous cytoskeleton. *In* Functional Epithelial Cells in Culture. K. S. Matlin and J. D. Valentich, editors. Alan R. Liss, Inc., New York. 3–42.

Ojakian, G. K., and R. Schwimmer. 1988. The polarized distribution of an apical cell surface glycoprotein is maintained by interactions with the cytoskeleton of Madin-Darby canine kidney cells. *J. Cell Biol.* 107:2377–2387.

Palek, J. 1987. Hereditary elliptocytosis, spherocytosis, and related disorders: consequences of a deficiency or a mutation of membrane skeletal proteins. *Blood Rev.* 1:147–168.

Palek, J., and S. E. Lux. 1983. Red cell membrane skeletal defects in hereditary and acquired hemolytic anemias. *Semin. Hematol.* 20:189–224.

Peterson, L. C., C. Dampier, T. Coetzer, J. Lawler, J. White, and J. Palek. 1987. Clinical and laboratory study of two Caucasian families with hereditary pyropoikilocytosis and hereditary elliptocytosis. *Am. J. Clin. Pathol.* 88:58–65.

Press, W. H., B. P. Flannery, S. A. Teukolsky, and W. T. Vetterling. 1986. Numerical Recipes: The Art of Scientific Computing. Cambridge University Press, Cambridge. 305–306.

Roux, S., and A. Hansen. 1988. Transfer-matrix study of the elastic properties of central-force percolation. *Europhys. Lett.* 6:301–306.

Saxton, M. J. 1989*a*. The spectrin network as a barrier to lateral diffusion in erythrocytes: a percolation analysis. *Biophys. J.* 55:21–28.

Saxton, M. J. 1989*b*. Lateral diffusion in an archipelago: distance dependence of the diffusion coefficient. *Biophys. J.* 56:615–622.

Saxton, M. J. 1990. The membrane skeleton of erythrocytes: models of its effect on lateral diffusion. *Int. J. Biochem.* In press.

Schwartz, L. M., S. Feng, M. F. Thorpe, and P. N. Sen. 1985. Behavior of depleted elastic networks: comparison of effective-medium and numerical calculations. *Phys. Rev. B.* 32:4607–4617.

Schwartz, R. S., A. C. Rybicki, R. H. Heath, and B. H. Lubin. 1987. Protein 4.1 in sickle erythrocytes. *J. Biol. Chem.* 262:15666–15672.

Shahbakhti, F., and W. B. Gratzer. 1986. Analysis of the self-association of human red cell spectrin. *Biochemistry*. 25:5969–5975.

Sheetz, M. P. 1983. Membrane skeletal dynamics: role in modulation of red cell deformability, mobility of transmembrane proteins, and shape. *Semin. Hematol.* 20:175–188.

Sheetz, M. P., and J. Casaly. 1980. 2,3-Diphosphoglycerate and ATP dissociate erythrocyte membrane skeletons. *J. Biol. Chem.* 255:9955–9960.

Sheetz, M. P., M. Schindler, and D. E. Koppel. 1980. Lateral mobility of integral membrane proteins is increased in spherocytic erythrocytes. *Nature (Lond.)*. 285:510–512.

Shen, B. W. 1989. Ultrastructure and function of membrane skeleton. *In* Red Blood Cell Membranes: Structure, Function, Clinical Implications. P. Agre and J. C. Parker, editors. Marcel Dekker, Inc., New York. 261–297.

Shields, M., P. La Celle, R. E. Waugh, M. Scholz, R. Peters, and H. Passow. 1987. Effects of intracellular Ca^{2+} and proteolytic digestion of the membrane skeleton on the mechanical properties of the red blood cell membrane. *Biochim. Biophys. Acta.* 905:181–194.

Smith, D. K., and J. Palek. 1983. Sulfhydryl reagents induce altered spectrin self-association, skeletal instability, and increased thermal sensitivity of red cells. *Blood.* 62:1190–1196.

Speicher, D. W., and V. T. Marchesi. 1984. Erythrocyte spectrin is comprised of many homologous triple helical segments. *Nature (Lond.)*. 311:177–180.

Stauffer, D. 1985. Introduction to Percolation Theory. Taylor and Francis, London. 124 pp.

Steck, T. L. 1974. The organization of proteins in the human red blood cell membrane. *J. Cell Biol.* 62:1–19.

Stokke, B. T., A. Mikkelsen, and A. Elgsaeter. 1985. Human erythrocyte spectrin dimer intrinsic viscosity: temperature dependence and implications for the molecular basis of the erythrocyte membrane free energy. *Biochim. Biophys. Acta.* 816:102–110.

Tsuji, A., and S. Ohnishi. 1986. Restriction of the lateral motion of band 3 in the erythrocyte membrane by the cytoskeletal network: dependence on spectrin association state. *Biochemistry*. 25:6133–6139.

Tsuji, A., K. Kawasaki, S. Ohnishi, H. Merkle, and A. Kusumi. 1988. Regulation of band 3 mobilities in erythrocyte ghost membranes by protein association and cytoskeletal meshwork. *Biochemistry*. 27:7447–7452.

Waugh, R. E. 1987. Effects of inherited membrane abnormalities on the viscoelastic properties of erythrocyte membrane. *Biophys. J.* 51:363–369.

Waugh, R. E., and P. Agre. 1988. Reductions of erythrocyte membrane viscoelastic coefficients reflect spectrin deficiencies in hereditary spherocytosis. *J. Clin. Invest.* 81:133–141.

Wolfe, L. C., A. M. Byrne, and S. E. Lux. 1986. Molecular defect in the membrane skeleton of blood bank-stored red cells. Abnormal spectrin-protein 4.1-actin complex formation. *J. Clin. Invest.* 78:1681–1686.

Zail, S. 1986. Clinical disorders of the red cell membrane skeleton. *CRC Crit. Rev. Oncol. Hematol.* 5:397–453.